

Characterizing Ligand-Gated Ion Channel Receptors with Genetically Encoded Ca^{++} Sensors

John G. Yamauchi^{1,2}, Ákos Nemezc^{1,3}, Quoc Thang Nguyen^{4*}, Arnaud Muller⁴, Lee F. Schroeder⁴, Todd T. Talley¹, Jon Lindstrom⁵, David Kleinfeld⁴, Palmer Taylor^{1*}

1 Department of Pharmacology, Skaggs School of Pharmacy and Pharmaceutical Sciences, University of California San Diego, La Jolla, California, United States of America, **2** Biomedical Sciences Graduate Program, University of California San Diego, La Jolla, California, United States of America, **3** Department of Chemistry and Biochemistry, University of California San Diego, La Jolla, California, United States of America, **4** Department of Physics, University of California San Diego, La Jolla, California, United States of America, **5** Department of Neurosciences, School of Medicine, University of Pennsylvania, Philadelphia, Pennsylvania, United States of America

Abstract

We present a cell based system and experimental approach to characterize agonist and antagonist selectivity for ligand-gated ion channels (LGIC) by developing sensor cells stably expressing a Ca^{2+} permeable LGIC and a genetically encoded Förster (or fluorescence) resonance energy transfer (FRET)-based calcium sensor. In particular, we describe separate lines with human $\alpha 7$ and human $\alpha 4\beta 2$ nicotinic acetylcholine receptors, mouse 5-HT_{3A} serotonin receptors and a chimera of human $\alpha 7$ /mouse 5-HT_{3A} receptors. Complete concentration-response curves for agonists and Schild plots of antagonists were generated from these sensors and the results validate known pharmacology of the receptors tested. Concentration-response relations can be generated from either the initial rate or maximal amplitudes of FRET-signal. Although assaying at a medium throughput level, this pharmacological fluorescence detection technique employs a clonal line for stability and has versatility for screening laboratory generated congeners as agonists or antagonists on multiple subtypes of ligand-gated ion channels. The clonal sensor lines are also compatible with *in vivo* usage to measure indirectly receptor activation by endogenous neurotransmitters.

Citation: Yamauchi JG, Nemezc Á, Nguyen QT, Muller A, Schroeder LF, et al. (2011) Characterizing Ligand-Gated Ion Channel Receptors with Genetically Encoded Ca^{++} Sensors. PLoS ONE 6(1): e16519. doi:10.1371/journal.pone.0016519

Editor: Mark Mattson, National Institute on Aging Intramural Research Program, United States of America

Received: November 26, 2010; **Accepted:** December 21, 2010; **Published:** January 28, 2011

Copyright: © 2011 Yamauchi et al. This is an open-access article distributed under the terms of the Creative Commons Attribution License, which permits unrestricted use, distribution, and reproduction in any medium, provided the original author and source are credited.

Funding: This work was funded by National Institutes of Health (NIH) grants R01-GM18360-39, U01-DA019372 (PT), and R01-DA029706 (DK). AN and JGY acknowledge support by training grant GM-07752. JGY also acknowledges support from NSF GK-12 0742551. The funders had no role in study design, data collection and analysis, decision to publish, or preparation of the manuscript.

Competing Interests: The author Quoc Thang Nguyen has since become employed at NeurAccel Biosciences.

* E-mail: pwtaylor@ucsd.edu

† Current address: NeurAccel Biosciences, La Jolla, California, United States of America

Introduction

Nicotinic acetylcholine receptors (nAChRs) are pentameric ligand-gated ion channels (LGIC) belonging to the sub-family of Cys-loop receptors. They are found in the central and peripheral nervous systems of both vertebrate and invertebrate species. Specific nAChR subtypes are recognized pharmaceutical targets for many central nervous system (CNS) diseases and conditions [1]. For example: the $\alpha 7$ -nAChR is targeted for schizophrenia [2], Alzheimer's disease [3], and cognition enhancement [4], and the $\alpha 4\beta 2$ -nAChR is also targeted for Alzheimer's disease [5,6], and for tobacco addiction [7,8]. Therefore, a particular challenge in therapeutic considerations is achieving subtype selectivity among the nAChRs. Sorting out the desirable actions within the subunit diversity of the nAChR family from the largely unwanted responses, via off-target receptors, is an important facet of the therapeutic approach [9].

For selection of pharmacologic leads, a facilitated and rapid assay of nAChR subtype selective agents is required early on in the screening process [10]. While electrophysiological methods through whole cell recording and patch clamp analysis can subsequently be used to uncover mechanism, they lack the scalability, cost reduction and automation that can be attained

through the use of photon generated signals from multi-well plates [11,12]. The scalability and automation derived from fluorometric imaging plate readers (FLIPR) have encouraged the use of fluorescence-based dyes in screening therapeutics on nAChRs [13,14]. Yet conventional fluorescent dyes to detect depolarization or intracellular calcium, are limited by cost, variations in dye administration, dye shelf life, and cell perturbations during injection. Hence a stable, clonal cell line containing a light detection sensor and a receptor, which is generated from incorporating the respective genetic material, become critical considerations in developing a medium throughput assay for selective receptor activation. Bioluminescent Ca^{2+} reporters, such as GFP-aequorin, have been shown to be an applicable method in creating cell lines that contain a genetically encoded light detection method [15,16]. Although bioluminescent reporters address the issues of variations in dye administration, shelf life, and cost; they are still susceptible to cell perturbations during injection, interference from fluorescent ligands, and are limited in time resolution due to the length of their decay. Applications that take advantage of fusing fluorescent protein Förster (or fluorescence) resonance energy transfer (FRET) pairs with Ca^{2+} binding proteins, such that changes in intracellular Ca^{2+} levels can be visualized through a combination of donor quenching and

acceptor sensitization, have become a prevalent method for enabling investigators to monitor signal transduction pathways in varying cells [17]. The use of FRET pairs over Ca^{2+} sensing bioluminescent reporters minimizes the perturbations of ligand fluorescence and cell perturbation by solvent during the injection phase. Although many genetically encoded Ca^{2+} sensors exist [18,19], the development of the Ca^{2+} sensor TN-XXL allowed for a highly sensitive and effective FRET based sensor [20]. Its incorporation with over-expressed G-protein-coupled receptors (GPCR) to produce cell-based neurotransmitter fluorescent engineered reporters (CNiFERS) offered the potential to overcome most of the limitations of the Ca^{2+} bioluminescent reporters [21]. In our previous studies, the generation of a genetically encoded sensitive Ca^{2+} sensor with a stably over-expressed GPCR allowed for *in vivo* validation of a compound's activity *in situ* in brain [21]. High-throughput fluorescence methodology [14], which has been previously utilized, affords a dual application to the stable, clonal cell line sensors we generated for transplanted cells. Here we report on generating and utilizing nAChR CNiFERS to measure nAChR activation via Ca^{2+} flux through ion channels in the cell membrane as opposed to GPCR mediated release primarily from intracellular stores described previously (Figure 1). Our studies extend the application of CNiFERS to prevalent and targeted CNS nAChR subtypes, the $\alpha 7$ and $\alpha 4\beta 2$, and also the 5-HT_{3A} serotonin receptor. A chimaeric receptor CNiFER composed of $\alpha 7/5\text{-HT}_{3A}$ was also generated to gain additional insight into activation of the wildtype $\alpha 7$ -nAChR. The chimaeric receptor has been shown to have a desensitization rate comparable to 5-HT_{3A} receptors, and more recently a higher conducting variant has been created [22,23,24]. This chimaeric receptor still maintains ligand affinities for that of the full-length $\alpha 7$ -nAChR, which allows for a positive allosteric modulator (PAM) free study of the $\alpha 7$ -nAChR [23]. We report on a cell-based assay incorporating the use of nAChR CNiFERS to identify and characterize nAChR agonists and antagonists with a low cost, medium throughput fluorescence assay. The system is capable of detection on a monolayer of cells in a 7 mm diameter well of a 96-well plate and has the potential to be scaled to a high throughput platform.

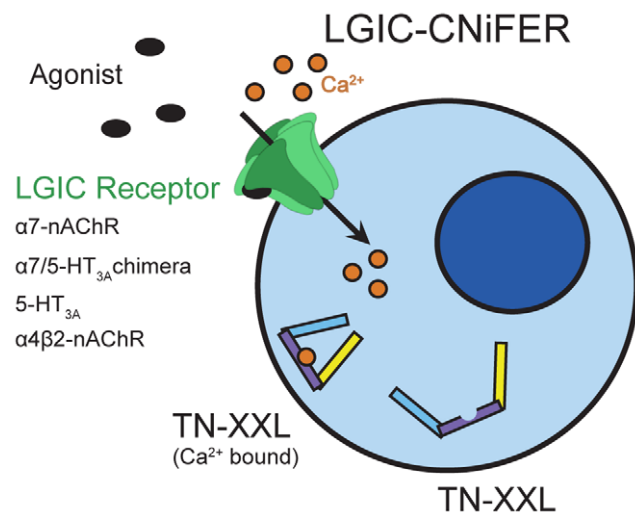


Figure 1. Simplistic representation of LGIC-CNIFERs and their response. Upon activation of a calcium permeable receptor, Ca^{2+} enters the cell and upon binding to TN-XXL produces a conformational change eliciting a fluorescence change reflected in quenching of the donor fluorescence and excitation of the acceptor.
doi:10.1371/journal.pone.0016519.g001

Results and Discussion

Cell Based Neurotransmitter Fluorescent Engineered Reporters (CNiFERS)

The first CNiFERS were developed for applications of monitoring cortical acetylcholine release in the cerebral cortex of rats using the M1-CNiFER [21]. The CNiFERS presented here were developed to facilitate pharmacological screening, potency rank ordering and characterization of compounds for calcium permeable ligand-gated ion channels (LGICs), with a particular focus on the homomeric $\alpha 7$ and heteromeric $\alpha 4\beta 2$ nAChRs. The 5-HT_{3A} serotonergic LGIC receptor exists in its simplest form as a homopentamer similar to the $\alpha 7$ -nAChR [25]. Although the 5-HT_{3A} receptor has a large calcium conductance, the 5-HT_{3AB} heteromeric receptors do not and therefore may have limited applicability with this technique [26]. Since antagonists, such as tropisetron, for the 5-HT_{3A} receptor are known to activate $\alpha 7$ -nAChRs, 5-HT_{3A} CNiFERS not only expand the neurotransmitter target base, but also become a model system for testing opposing receptor responses [27]. LGIC agonist responses were measured with CNiFERS by monitoring TN-XXL FRET ratios, emissions of citrine cp174 (527 nm) to eCFP (485 nm), over 120 seconds with agonist injections occurring at the 30 second timepoint. Figure 2a is an example of the fluorescent signals generated from a 5-HT_{3A} CNiFER single concentration response to 3 μM 5-Hydroxytryptamine (5-HT) injected at 30 seconds. FRET ratios of the emissions for a concentration range of 0.3–3 μM 5-HT is shown in Figure 2b. Concentration response curves can then be generated from the peak FRET ratio values for each concentration.

$\alpha 7$ -nAChR CNiFERS

Due to the rapid rate of desensitization of the $\alpha 7$ -nAChR in the time frame of milliseconds [28], monitoring agonist-elicited fluorescence responses were not possible without including a PAM [29]. In our case we used the type II PAM, N-(5-Chloro-2,4-dimethoxyphenyl)-N'-(5-methyl-3-isoxazolyl)-urea (PNU-120596), and found that concentrations of 10 μM and above incubated on cells for at least 30 min (data not shown) yielded a maximal agonist-elicited fluorescence response (Figure 3a). Characteristic of a type II PAM, PNU-120596 will increase ion flux through the $\alpha 7$ -nAChRs by decreasing its desensitization rate [30]. PNU-120596 likely interacts with a region in the transmembrane helices spanning TM1, TM2, and TM4 to prevent an activated $\alpha 7$ -nAChR from switching to its desensitized state once activated [31]. PNU-120596 modulating activity results in an increase in the number of receptors remaining in an open or activated state. Accordingly, not only is a larger response produced, but also a lower concentration of agonist is likely needed to observe a response. Agonist EC₅₀ values measured with the $\alpha 7$ -nAChR CNiFER in the presence of PNU-120596 are less than those reported in the literature for $\alpha 7$ -nAChR agonists without PNU-120596, as observed in Table 1. Nevertheless, these considerations are not likely to affect the rank ordering for agonist potencies. Assay of antagonists is conducted as a null method and should be independent of agonist used, provided a single receptor subtype is being analyzed. When (\pm)-epibatidine responses from $\alpha 7$ -nAChR CNiFERS were blocked with three concentrations (3, 10, 30 nM) of methyllycaconitine (MLA) (Figure 3b). Schild analysis of the parallel concentration versus fluorescence readout showed MLA to block $\alpha 7$ -nAChR CNiFERS competitively with a slope of -1.2 ± 0.3 and with an observed K_a value of 3.2 ± 1.4 nM for the antagonist (Figure 3c, Table 2).

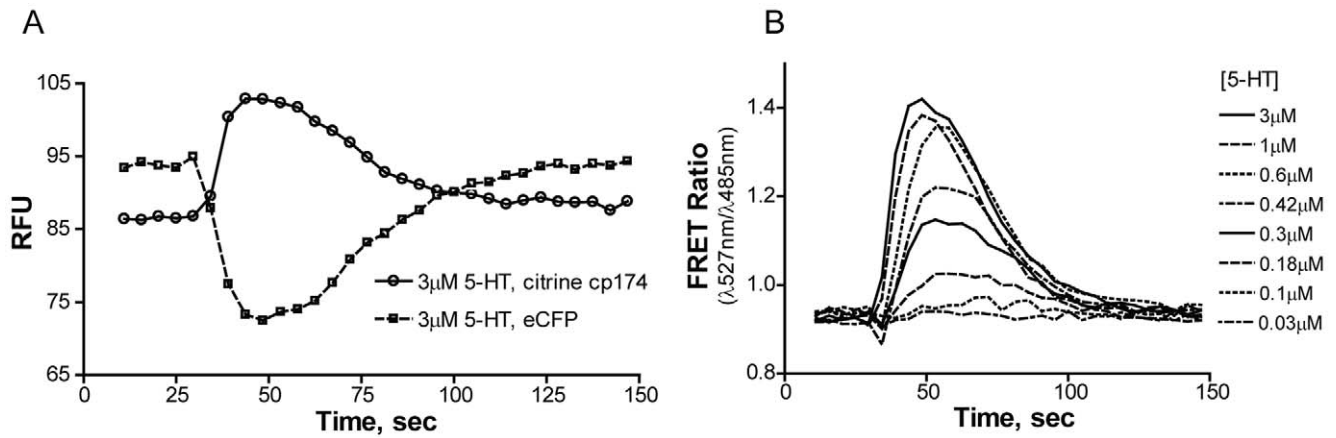


Figure 2. Direct FRET measurement of response. A. Measured time-course emission wavelengths for eCFP (485 nm) and Citrine cp174 (527 nm) on 5-HT_{3A} CNiFERS. 5-HT was injected at 30 s at 3 μM concentration to produce a Ca²⁺ influx causing a concentration dependent FRET response from the TN-XXL reporter. Measurements were taken every 3.52 s with excitation at 436 nm. B. FRET-Ratio (Citrine cp147/eCFP) time-course responses from 5-HT_{3A} CNiFERS to varying concentrations of 5-HT. Peak values or initial rates may be used to plot a concentration dependent curve to estimate EC₅₀ values. Peak values were used to generate concentration response curves. doi:10.1371/journal.pone.0016519.g002

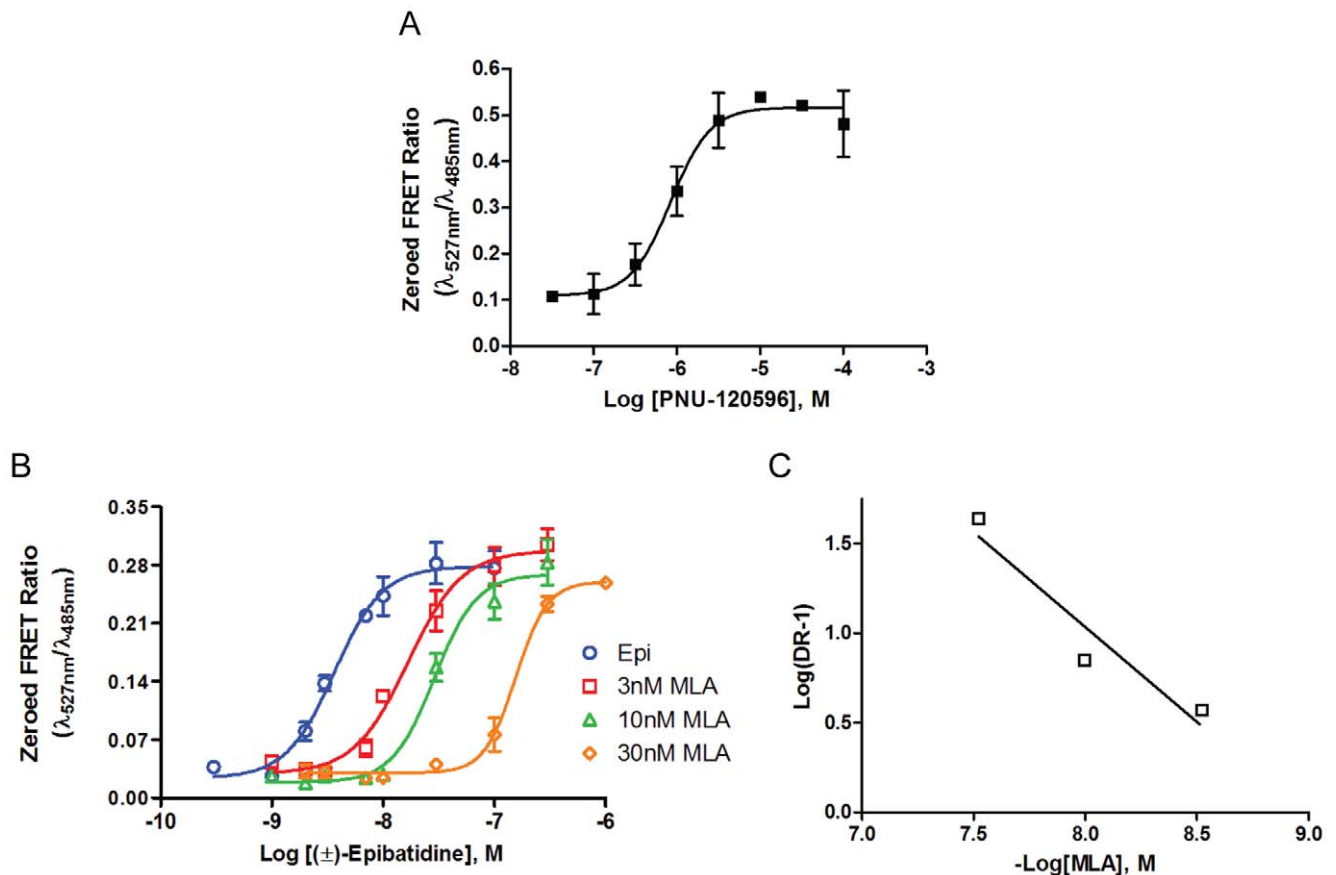


Figure 3. α7-nAChR CNiFER: PNU-120596 activation and methyllycaconitine antagonism. A. Concentration dependent response of PNU-120596 incubated for 30 minutes on α7-nAChR CNiFERS and stimulated with 0.1 μM (±)-epibatidine. The response curve shows that concentrations greater than 10 μM PNU-120596 would produce a maximal response. B. Competitive blockade of (±)-epibatidine elicited responses on α7-nAChR CNiFERS by MLA. The EC₅₀ values for each curve shifted from 3.6 nM to 17 nM, 29 nM, and 160 nM for 3 nM, 10 nM, 30 nM MLA respectively. C. Schild plot of concentration dependent shifts. A slope of -1.2 ± 0.3 confirmed MLA to block competitively. doi:10.1371/journal.pone.0016519.g003

Table 1. Comparison of Agonist EC₅₀ using CNiFER and non-CNiFER detection^f.

	$\alpha 7/5\text{-HT}_{3A}$ CNiFER	$\alpha 7/5\text{-HT}_{3A}$	$\alpha 7\text{-nAChR}$ CNiFER	$\alpha 7\text{-nAChR}$	$\alpha 4\beta 2\text{-nAChR}$ CNiFER	$\alpha 4\beta 2\text{-nAChR}$
(\pm)-Epibatidine (EC ₅₀ , nM)	250 \pm 50 (n = 5) ^a	180 \pm 20 ^b	28 \pm 16 (n = 24) ^c	17 \pm 2.6 ^d	14 \pm 9 (n = 17) ^a	27 \pm 6 (n = 6) ^d
(-)-Nicotine (EC ₅₀ , nM)	10,000 \pm 2,600 (n = 3) ^a	19,100 \pm 7,300 ^b	410 \pm 270 (n = 10) ^c	1,160 \pm 180 ^{d†} , 92 \pm 12 ^e	1,850 \pm 810 (n = 4) ^a	2,700 \pm 200 ^{d†} , 3,500 ^{b†}

a. Measured in aCSF.

b. Measured with Ca²⁺ dye (Fluo-3-AM) on HEK293 cells expressing human receptors [23] *(Geometric Mean[-SD = 2.4, +SD = 5.1])[39].

c. Measured with 10 μ M PNU-120596 in aCSF.

d. Measured with potential-sensitive dye against human receptors. *(2 α 3 β) [35].

e. Measured with potential-sensitive dye and 3 μ M PNU-120596.

†To be published Kuryatov A, Mukherjee J, and Lindstrom J.

f. Each n is calculated as an EC₅₀ value from an individual concentration-response curve.

doi:10.1371/journal.pone.0016519.t001

$\alpha 7/5\text{-HT}_{3A}$ Chimaeric Receptor CNiFER

The chimaeric $\alpha 7/5\text{-HT}_{3A}$ receptor does not exhibit the rapid desensitization rate seen with the wildtype (wt) $\alpha 7\text{-nAChR}$ and thus neither requires PNU-120596, nor would PNU-120596 be effective [31], for achieving sufficient fluorescence signals within the time frame of the assay. In the presence of PNU-120596, agonists tend to have approximately a 10-fold higher affinity for the $\alpha 7\text{-nAChR}$ (Table 1). The EC₅₀ value for (\pm)-epibatidine measured in the presence of PNU-120596 for $\alpha 7\text{-nAChR}$ CNiFERs was 28 \pm 16 nM, whereas the EC₅₀ value measured without PNU-120596 on $\alpha 7/5\text{-HT}_{3A}$ CNiFERs was 250 \pm 50 nM. In this case the chimaeric $\alpha 7/5\text{-HT}_{3A}$ receptor can possibly yield measurements of potency closest to the actual channel opening event of the compound for the wt $\alpha 7\text{-nAChR}$. This difference may reflect affinity differences between the activatable and desensitized state of the receptor originally shown in the muscle nAChR [32]. Concentration-response curves generated with (\pm)-epibatidine on $\alpha 7/5\text{-HT}_{3A}$ CNiFERs were blocked with MLA (3, 10, 30 nM) to characterize MLA antagonism. The resulting shifts were similar to those seen with the $\alpha 7\text{-nAChR}$ CNiFERs (Figure 4a). The decrease in the maximum responses in the presence of MLA (Figure 4a) was also seen on several occasions with the $\alpha 7\text{-nAChR}$ CNiFERs. This suggests a non-competitive component of antagonism, or that the half time of 2.3 min for dissociation of MLA is too slow to allow for complete dissociation from the receptor in the timeframe of our measurements [33]. Schild analysis showed a slope of -1.8 ± 0.2 , which indicates that MLA is not solely a competitive antagonist at the $\alpha 7/5\text{-HT}_{3A}$ CNiFERs (Figure 4b). However, the major competitive component yielded a K_a of 2.5 \pm 0.1 nM, a value very close to that measured on the $\alpha 7\text{-nAChR}$ CNiFERs (Table 2).

The similarity of the antagonist affinities shows that using a PAM only affects agonist constants and employing the null method for determining K_a values negates the effect of PAMs. The similarity of these values for occupation by the antagonist validates the use of these chimaeric $\alpha 7/5\text{-HT}_{3A}$ CNiFERs for characterizing ligands for the $\alpha 7\text{-nAChR}$ without the need to use a PAM. Antagonist binding is more apt to be characterized by a single binding state as shown with the muscle nAChRs [34].

$\alpha 4\beta 2\text{-nAChR}$ CNiFERs

To characterize the $\alpha 4\beta 2\text{-nAChR}$ CNiFERs, concentration-response relationship data were generated with various concentrations of (\pm)-epibatidine in the absence and presence of a known competitive antagonist, dihydro-beta-erythroidine (DH β E) (0.3, 1, 3 μ M). The resulting concentration-response curves showed a parallel shift with little decrease in the maximum revealing competitive antagonism (Figure 5a). Schild analysis confirmed DH β E acts competitively with a slope of -0.9 ± 0.1 and measured a K_a value of 136 \pm 54 nM (Figure 5b, Table 2).

5-HT_{3A} Serotonin CNiFERs

The 5-HT_{3A} receptor was generated from a single transfected subunit to form a homomeric pentamer. Concentration-response curves show serotonin to be an agonist, as expected, with an EC₅₀ of 349 \pm 78 nM (n = 16). A near competitive block is achieved with ondansetron as an antagonist (Figure 6, Table 2). Other sertrons, such as tropisetron and granisetron appear to show a greater non-competitive component (data not shown), but this observation may result from slow dissociation of the antagonist during the agonist

Table 2. Comparison of Antagonist K_a from CNiFERs to non-CNiFERs detection^f.

LGIC-CNIFER	Antagonist	CNiFER K _a , nM	Schild Slope	IC ₅₀ , nM
$\alpha 7\text{-nAChR}$	MLA	3.2 \pm 1.4 ^a (n = 6)	-1.2 \pm 0.3	2.9 \pm 1.2 ^c
$\alpha 7/5\text{-HT}_{3A}$	MLA	2.5 \pm 0.1 ^b (n = 2)	-1.8 \pm 0.2	36 \pm 13 ^d
$\alpha 4\beta 2\text{-nAChR}$	DH β E	136 \pm 54 ^b (n = 5)	-0.9 \pm 0.1	88 \pm 24 ^{c†} , 85(K _b) ^{d†}
5-HT _{3A}	Ondansetron	1.6 \pm 0.9 ^b (n = 7)	-1.3 \pm 0.04	16.0 \pm 5.7(K _i) ^e

a. Measured with 10 μ M PNU-120596 in aCSF.

b. Measured in aCSF.

c. Measured with potential-sensitive dye (to be published Kuryatov A, Mukherjee J, and Lindstrom J). *(2 α 3 β) [40].

d. Measured with Ca²⁺ dye (Fluo-3-AM) on HEK293 cells expressing human receptors [23]. *(Geometric Mean [-SD = 66, +SD = 109])[39].

e. Measured competition against [³H]-ICs-205-930 in mouse neuroblastoma-glioma cells (NG-108-15) (5-HT_{3A}) [41,42].

f. Each n is calculated from a Schild regression plot.

doi:10.1371/journal.pone.0016519.t002

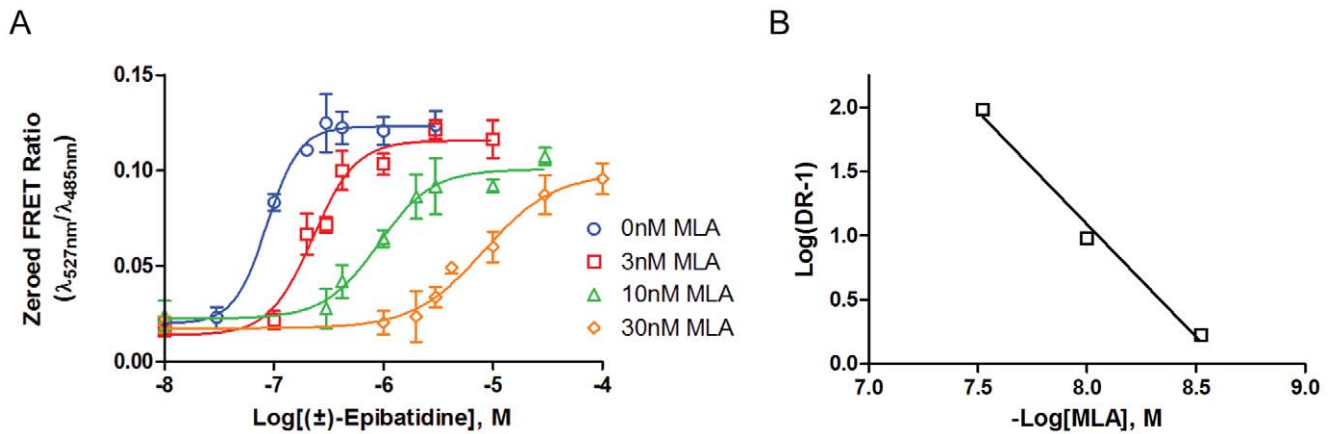


Figure 4. $\alpha 7/5\text{-HT}_{3A}$ CNiFER: Methyllycaonitine antagonism. A. Competitive blockade of (\pm)-epibatidine elicited responses on $\alpha 7/5\text{-HT}_{3A}$ CNiFERs by MLA. The EC_{50} values for each curve shifted from 86 nM to 230 nM, 900 nM, and 8.3 μ M for 3 nM, 10 nM, 30 nM MLA respectively. B. Schild plot of concentration dependent shifts. A slope of -1.8 ± 0.2 shows MLA to block competitively but with a percentage of receptors still occupied, attributing to a slight non-competitive component that may be an artifactual result of slow dissociation. doi:10.1371/journal.pone.0016519.g004

exposure interval, as previously mentioned with MLA on the $\alpha 7$ -nAChR.

Concluding Analysis

CNiFER detection of agonist responses and blockade of the responses by antagonists, originally shown for a GPCR, muscarinic M1 receptor, are equally applicable to calcium permeable ligand-gated ion channels, as shown here for subunits of the Cys-loop receptor family. The chief advantages stem from the versatility of the system enabling one to measure responses to a variety of receptors in the same family by multi-array analysis. By developing the assay in a clonal cell line in which stable lines were first generated from the receptor subtype followed by plasmid transfection, or transduction with a viral vector containing the recombinant DNA encoded sensor, one can robustly generate previously established receptor subtype clones containing the FRET based sensor. These sensor clones may be used for either a robust medium-throughput assay or for *in vivo* implantation to determine neurotransmitter release [21]. The Molecular Devices FlexStation III instrument allows for multiple well samples in a 96

well plate to be assayed over 30 min plate intervals. This method could be scaled for use with higher throughput assaying via the FLIPR, or even for integration with high content screening platforms. Comparison of LGIC CNiFERs to their non-CNiFER counterparts shows similar ligand affinities and demonstrates that the TN-XXL sensor does not affect LGIC dissociation constants (Table 2). Our demonstration of (\pm)-epibatidine and 5-HT-elicited responses with predicted concentration ratio shifts from well known competitive antagonists provides a characterized cell system to distinguish defined receptor responses from indirect actions. We establish the utility of the CNiFER sensor for characterizing agonist and antagonist parameters for new ligand candidates on LGIC nicotinic and serotonin systems.

A chief limitation is the slow read time between measurements and the sensitivity of the sensor, resulting in difficulty with fast desensitizing receptor systems; yet with the judicious use of agents that maintain an active state and retard desensitization, this obstacle may be overcome and a suitable rank ordering of potency determined for agonists and antagonists. Distortions that might be achieved with more prolonged measurements of maximal

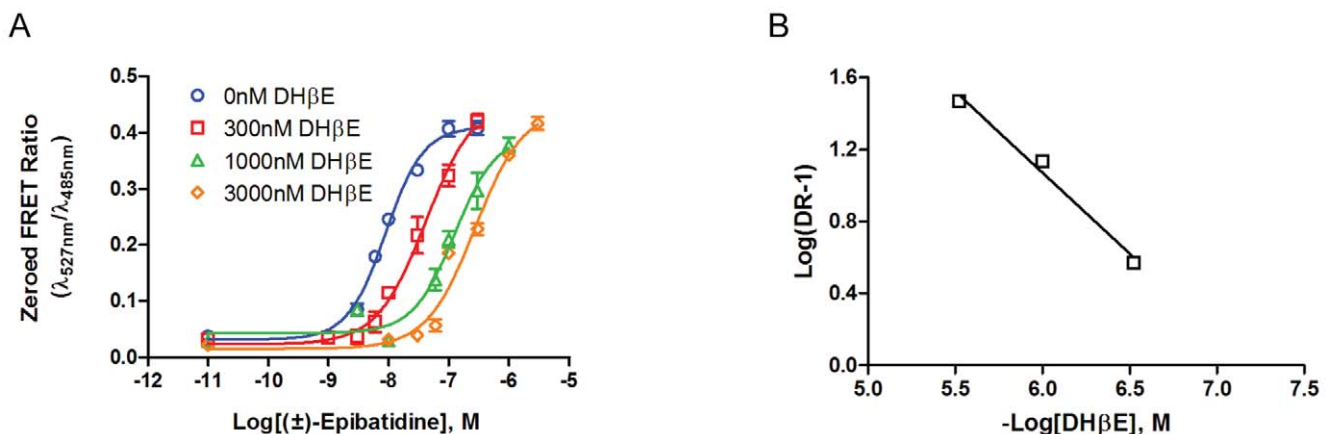


Figure 5. $\alpha 4\beta 2$ -nAChR CNiFER: DH β E antagonism. A. Competitive blockade of (\pm)-epibatidine elicited responses on $\alpha 4\beta 2$ -nAChR CNiFERs by DH β E. The EC_{50} values for each curve shifted from 8.9 nM to 42 nM, 130 nM, and 270 nM for 300 nM, 1 μ M, 3 μ M DH β E respectively. B. Schild plot of concentration dependent shifts. A slope of -0.9 ± 0.1 confirmed DH β E to block competitively. doi:10.1371/journal.pone.0016519.g005

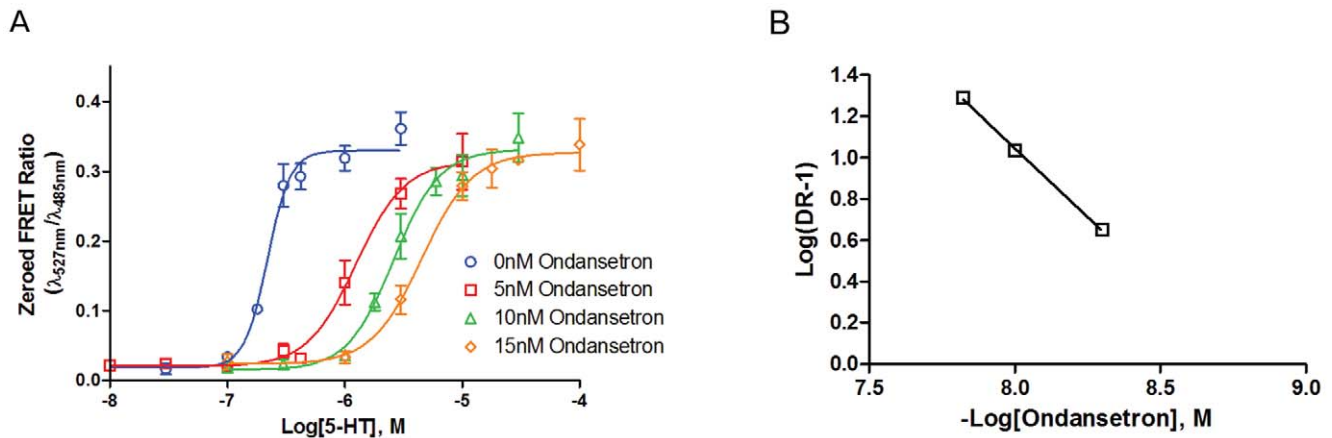


Figure 6. 5-HT_{3A} CNiFER: Ondansetron antagonism. A. Competitive blockade of 5-HT elicited responses on 5-HT_{3A} CNiFERs by ondansetron. The steep Hill coefficient of 2.6 shows the more cooperative nature of the 5-HT_{3A} receptor. The EC₅₀ values for each curve shifted from 220 nM to 1.6 μ M, 2.6 μ M, and 4.5 μ M for 5 nM, 10 nM, 15 nM ondansetron respectively. B. Schild plot of concentration dependent shifts. A slope of -1.3 ± 0.04 confirmed ondansetron to block competitively. doi:10.1371/journal.pone.0016519.g006

depolarization can be minimized through monitoring the initial rate of depolarization. The slow off-rate antagonists that reduce signal and reveal an artifactual non-competitive component to antagonism exhibit another limitation from the reported on assay. By analyzing only the competitive aspect of the compound, one can effectively estimate K_a values. Therefore the use of LGIC CNiFERs in the development of therapeutics for CNS disorders is robust and cost-effective.

Methods

Generation of Stable Ca²⁺ Sensing nAChR Cell Lines

Individual HEKtsA201 human $\alpha 4\beta 2$ nicotinic receptor stable cell lines were generated as previously described [35]. Briefly human cDNA clones encoding $\alpha 4$ (pcDNA3.1/Zeo(-)) and $\beta 2$ (pRc/CMV) nAChR subunits were transfected in equal amounts into HEKtsA201 cells using the FuGene6 transfection agent (Roche Diagnostics, Indianapolis, IN). Zeocin (0.5 mg/ml) was used for selection of $\alpha 4$ expression, and G418 (0.6 mg/ml; both from Invitrogen, Carlsbad, CA) was used for $\beta 2$ selection to produce a stable, clonal cell line. Selection of the HEKtsA201 human $\alpha 7$ -Ric3 nicotinic receptor stable cell lines and their pharmacological properties has been reported by Kuryatov, Mukherjee, and Lindstrom. The basic approach to preparing the line was similar to that used for the $\alpha 4\beta 2$ -nAChR cell line and its functional properties were similarly assayed using a potential-sensitive indicator after treatment with chemical chaperones to upregulate the amount of AChR. The stable clones were used to generate individual nAChR CNiFERs. The TN-XXL control CNiFERs (lacking over-expressed receptors) [20,21], and mouse 5-HT_{3A} CNiFERs were developed as described in [21]. TN-XXL gene expression was introduced into each of the $\alpha 7$ -Ric3 and $\alpha 4\beta 2$ cells via lentiviral transduction as described [21] and fluorescence activated cell sorted (FACS) for high levels of eCFP and Citrine cp174 fluorescence. Chimaeric receptor DNA of human $\alpha 7(1-202)$ /mouse 5-HT_{3A} was kindly provided by Dr. Steven Sine (Mayo Clinic, Rochester, MN). The $\alpha 7/5$ -HT_{3A} chimaeric CNiFER was generated by calcium phosphate transfection of TN-XXL control cells with an $\alpha 7/5$ -HT_{3A} gene subcloned into pcDNA3.1+ containing 5-HT_{3A} conductance-enhancing mutations of R432Q, R436D, and R440A [36]. Stable selection was achieved using G418 (0.5 mg/ml) to yield a TN-XXL control cell,

as described in [21], containing over-expressed $\alpha 7/5$ -HT_{3A} receptors, which were then selected by FACS as noted above.

Flex Assay on Receptors

Cells were cultured in 10 cm plates with DMEM (Mediatech, Manassas, VA) supplemented with 10% FBS (Gemini Bio-Products, West Sacramento, CA; Atlanta Biologicals, Lawrenceville, GA) and 1% Glutamine (Invitrogen), and incubated at 37°C with 10% CO₂. Cells were selected at ~70% confluency and plated the day before using 100 μ l volumes per well into black, transparent flat-bottom, TC treated 96-well plates (Thermo, Waltham, MA; E&K, Greiner Campbell, CA). Plates were removed from the incubator the next day and the media was replaced with 100 μ l of artificial cerebral spinal fluid (aCSF) [containing 121 mM NaCl, 2.4 mM Ca²⁺, 1.3 mM Mg²⁺, 5 mM KCl, 26 mM NaHCO₃, 1.2 mM Na₂HPO₄, 10 mM glucose, 5 mM Hepes Na⁺, pH 7.4]. For all assays performed on $\alpha 7$ -nAChR CNiFERs 10 μ M of the PAM, PNU-120596 (Tocris, Ellisville, MO), was prepared in aCSF. In the case of antagonist measurements, antagonists, at 1.5 times the final desired concentration, were prepared in aCSF. For non-CNiFER cell lines, Blue Membrane Potential dye (Molecular Devices, Sunnyvale, CA) was prepared in aCSF and diluted 2 fold the recommended dilution. Plates were incubated for at least 30 min at 37°C and 10% CO₂ for any assay that included antagonist, dye, or PAM modification to the aCSF. Following incubation, plates were removed and placed into the Molecular Devices FlexStation III instrument and run at 37°C. Injection rates varied between 27–48 ml/s, and 50 μ l of the specified agonist prepared at 3x final concentration in the aforementioned aCSF solution was injected after 30 s of baseline measurement. Reads of both donor eCFP (485 nm) and acceptor Citrine cp174 (527 nm) emission with eCFP excitation (436 nm) were made at 3.52 s intervals as shown in Figure 2a, or for non-CNiFER experiments with blue membrane dye, 565 nm was read with an excitation of 530 nm, for 90–120 s depending on the experiment. FRET ratios of the two wavelengths were plotted as shown in Figure 2b, and the peak height or initial rate of ion flux for the well was used to determine EC₅₀ values for the injected agonist, acquired using SoftMax Pro 5.2 (Molecular Devices). All wells were replicated (two or three times) in the same plate. Mean peak FRET ratios calculated from

replicates were exported and plotted against agonist concentrations using Graphpad Prism 4 (Carlsbad, CA). A sigmoidal concentration-response (variable slope) regression of the mean peak FRET ratios was fit to generate a concentration-response curve and obtain an EC₅₀ value.

To measure potencies of competitive antagonists, three concentration-response curves with different antagonist concentrations were compared to a control curve (without antagonist). Mean FRET responses generated concentration response curves, and antagonist dependent shifts in EC₅₀ values were used to calculate dose ratios (DR), as a concentration ratio of EC₅₀'/EC₅₀ for the specified agonist (where EC₅₀' is in the presence of the antagonist at the specified concentration). DRs were used to produce a Schild regression plot for analysis of competitive antagonism and generate a K_a value. Analysis consisted of plotting Log (DR-1) against -Log [Antagonist]. The Schild K_a value for competitive antagonists was calculated from the x-intercept at

$y=0$, as the $-\text{Log}(K_a)$ [37,38]. All errors reported are arithmetic standard deviations unless otherwise noted.

Acknowledgments

The authors would like to thank Dr. Steven Sine for the donation of $\alpha 7/5$ -HT_{3A} cDNA and Wenru Yu for tissue culture expertise.

Author Contributions

Conceived and designed the experiments: JGY AN QTN AM LFS JL DK PT. Performed the experiments: JGY AN QTN LFS JL. Analyzed the data: JGY AN TTT JL PT. Contributed reagents/materials/analysis tools: JL DK PT. Wrote the paper: JGY AN PT. $\alpha 7/5$ HT_{3A}-CNiFER cell line design: JGY. $\alpha 7$, $\alpha 4\beta 2$ -CNiFER cell line design: JGY. AN 5-HT_{3A}-CNiFER cell line design: QTN LFS AM. Assay development and optimization: AN LFS. Non-CNiFER experimental work: JGY AN JL. Provided $\alpha 7$, $\alpha 4\beta 2$ cell line: JL. Manuscript edits and review: JGY AN QTN AM LFS JL DK PWT.

References

- Hogg RC, Raggenbass M, Bertrand D (2003) Nicotinic acetylcholine receptors: from structure to brain function. *Rev Physiol Biochem Pharmacol* 147: 1–46.
- Freedman R, Olincy A, Buchanan RW, Harris JG, Gold JM, et al. (2008) Initial phase 2 trial of a nicotinic agonist in schizophrenia. *Am J Psychiatry* 165: 1040–1047.
- Dziewczapolski G, Glogowski CM, Masliah E, Heinemann SF (2009) Deletion of the alpha 7 nicotinic acetylcholine receptor gene improves cognitive deficits and synaptic pathology in a mouse model of Alzheimer's disease. *J Neurosci* 29: 8805–8815.
- Young JW, Crawford N, Kelly JS, Kerr LE, Marston HM, et al. (2007) Impaired attention is central to the cognitive deficits observed in alpha 7 deficient mice. *Eur Neuropsychopharmacol* 17: 145–155.
- Newhouse PA, Potter A, Levin ED (1997) Nicotinic system involvement in Alzheimer's and Parkinson's diseases. Implications for therapeutics. *Drugs Aging* 11: 206–228.
- Warpman U, Nordberg A (1995) Epibatidine and ABT 418 reveal selective losses of alpha 4 beta 2 nicotinic receptors in Alzheimer brains. *Neuroreport* 6: 2419–2423.
- Salminen O, Murphy KL, McIntosh JM, Drago J, Marks MJ, et al. (2004) Subunit composition and pharmacology of two classes of striatal presynaptic nicotinic acetylcholine receptors mediating dopamine release in mice. *Mol Pharmacol* 65: 1526–1535.
- Maskos U, Molles BE, Pons S, Besson M, Guiard BP, et al. (2005) Nicotine reinforcement and cognition restored by targeted expression of nicotinic receptors. *Nature* 436: 103–107.
- Taly A, Corringier P, Guedin D, Lestage P, Changeux J-P (2009) Nicotinic receptors: allosteric transitions and therapeutic targets in the nervous system. *Nat Rev Drug Discov* 8: 733–750.
- Arneric SP, Holladay M, Williams M (2007) Neuronal nicotinic receptors: a perspective on two decades of drug discovery research. *Biochem Pharmacol* 74: 1092–1101.
- Dunlop J, Bowlby M, Peri R, Vasilyev D, Arias R (2008) High-throughput electrophysiology: an emerging paradigm for ion-channel screening and physiology. *Nat Rev Drug Discov* 7: 358–368.
- Sidach SS, Fedorov NB, Lippicello PM, Bencherif M (2009) Development and optimization of a high-throughput electrophysiology assay for neuronal alpha4beta2 nicotinic receptors. *J Neurosci Methods* 182: 17–24.
- Dunlop J, Roncarati R, Jow B, Bothmann H, Lock T, et al. (2007) In vitro screening strategies for nicotinic receptor ligands. *Biochem Pharmacol* 74: 1172–1181.
- Fitch RW, Xiao Y, Kellar KJ, Daly JW (2003) Membrane potential fluorescence: a rapid and highly sensitive assay for nicotinic receptor channel function. *Proc Natl Acad Sci U S A* 100: 4909–4914.
- Baubet V, Le Mouellie H, Campbell AK, Lucas-Meunier E, Fossier P, et al. (2000) Chimeric green fluorescent protein-aquorin as bioluminescent Ca²⁺ reporters at the single-cell level. *Proc Natl Acad Sci U S A* 97: 7260–7265.
- Drobac E, Tricoire L, Chaffotte AF, Guiot E, Lambolze B (2010) Calcium imaging in single neurons from brain slices using bioluminescent reporters. *J Neurosci Res* 88: 695–711.
- Kleinfeld D, Griesbeck O (2005) From art to engineering? The rise of in vivo mammalian electrophysiology via genetically targeted labeling and nonlinear imaging. *PLoS Biol* 3: e355.
- Mank M, Griesbeck O (2008) Genetically encoded calcium indicators. *Chem Rev* 108: 1550–1564.
- Miyawaki A (2005) Innovations in the imaging of brain functions using fluorescent proteins. *Neuron* 48: 189–199.
- Mank M, Santos AF, Dierenberger S, Mrcsic-Flogel TD, Hofer SB, et al. (2008) A genetically encoded calcium indicator for chronic in vivo two-photon imaging. *Nature Methods* 5: 805–811.
- Nguyen Q-T, Schroeder LF, Mank M, Muller A, Taylor P, et al. (2009) An in vivo biosensor for neurotransmitter release and in situ receptor activity. *Nature Neuroscience* 13: 127–132.
- Eisele JL, Bertrand S, Galzi JL, Devillers-Thiery A, Changeux JP, et al. (1993) Chimaeric nicotinic-serotonergic receptor combines distinct ligand binding and channel specificities. *Nature* 366: 479–483.
- Craig P, Bose S, Zwart R, Beattie R, Folly E, et al. (2004) Stable expression and characterisation of a human $\alpha 7$ nicotinic subunit chimera: a tool for functional high-throughput screening. *Eur J Pharmacol* 502: 31–40.
- Rayes D, Spitzmaul G, Sine SM, Bouzat C (2005) Single-channel kinetic analysis of chimeric alpha7-5HT_{3A} receptors. *Mol Pharmacol* 68: 1475–1483.
- Maricq AV, Peterson AS, Brake AJ, Myers RM, Julius D (1991) Primary structure and functional expression of the 5HT₃ receptor, a serotonin-gated ion channel. *Science* 254: 432–437.
- Davies PA, Pistis M, Hanna MC, Peters JA, Lambert JJ, et al. (1999) The 5-HT_{3B} subunit is a major determinant of serotonin-receptor function. *Nature* 397: 359–363.
- Papke R, Schiff H, Jack B, Horenstein N (2005) Molecular dissection of tropisetron, an $\alpha 7$ nicotinic acetylcholine receptor-selective partial agonist. *Neuroscience Letters* 378: 140–144.
- Bouzat C, Bartos M, Corradi J, Sine SM (2008) The interface between extracellular and transmembrane domains of homomeric Cys-loop receptors governs open-channel lifetime and rate of desensitization. *J Neurosci* 28: 7808–7819.
- Roncarati R, Seredenina T, Jow B, Jow F, Papini S, et al. (2008) Functional properties of $\alpha 7$ nicotinic acetylcholine receptors co-expressed with RIC-3 in a stable recombinant CHO-K1 cell line. *ASSAY Drug Dev Technol* 6: 181–193.
- Bertrand D, Gopalakrishnan M (2007) Allosteric modulation of nicotinic acetylcholine receptors. *Biochem Pharmacol* 74: 1155–1163.
- Young GT, Zwart R, Walker AS, Sher E, Millar NS (2008) Potentiation of 7 nicotinic acetylcholine receptors via an allosteric transmembrane site. *Proc Natl Acad Sci U S A* 105: 14686–14691.
- Sine S, Taylor P (1979) Functional consequences of agonist-mediated state transitions in the cholinergic receptor. Studies in cultured muscle cells. *J Biol Chem* 254: 3315–3325.
- Davies AR, Hardick DJ, Blagbrough IS, Potter RV, Wolstenholme AJ, et al. (1999) Characterisation of the binding of [³H]methyllycaconitine: a new radioligand for labelling alpha 7-type neuronal nicotinic acetylcholine receptors. *Neuropharmacol* 38: 679–690.
- Sine SM, Taylor P (1981) Relationship between reversible antagonist occupancy and the functional capacity of the acetylcholine receptor. *J Biol Chem* 256: 6692–6699.
- Kuryatov A, Luo J, Cooper J, Lindstrom J (2005) Nicotine acts as a pharmacological chaperone to up-regulate human alpha4beta2 acetylcholine receptors. *Mol Pharmacol* 68: 1839–1851.
- Kelley SP, Dunlop JI, Kirkness EF, Lambert JJ, Peters JA (2003) A cytoplasmic region determines single-channel conductance in 5-HT₃ receptors. *Nature* 424: 321–324.
- Taylor P, Insel PA (1990) Molecular basis of pharmacologic selectivity. Chapter 1. In: Pratt WB, Taylor P, eds. Principles of drug action: the basis of pharmacology 3rd Ed 3rd ed. New York: Churchill Livingstone. pp 1–102.
- Wyllie DJA, Chen PE (2009) Taking the time to study competitive antagonism. *Br J Pharmacol* 150: 541–551.
- Chavez-Noriega LE, Gillespie A, Stauderman KA, Crona JH, Claeps BO, et al. (2000) Characterization of the recombinant human neuronal nicotinic

- acetylcholine receptors $\alpha 3\beta 2$ and $\alpha 4\beta 2$ stably expressed in HEK293 cells. *Neuropharmacol* 39: 2543–2560.
40. Kuryatov A, Onksen J, Lindstrom J (2008) Roles of accessory subunits in $\alpha 4\beta 2$ (*) nicotinic receptors. *Mol Pharmacol* 74: 132–143.
 41. Rizzi JP, Nagel AA, Rosen T, McLean S, Seeger T (1990) An initial three-component pharmacophore for specific serotonin-3 receptor ligands. *J Med Chem* 33: 2721–2725.
 42. Rosen T, Nagel AA, Rizzi JP, Ives JL, Daffeh JB, et al. (1990) Thiazole as a carbonyl bioisostere. A novel class of highly potent and selective 5-HT₃ receptor antagonists. *J Med Chem* 33: 2715–2720.